

Heating of electrons in a superconductor in the resistive state by electromagnetic radiation

E. M. Gershenzon, M. E. Gershenzon, G. N. Gol'tsman, A. D. Semenov, and A. V. Sergeev

Moscow State Pedagogic Institute

(Submitted 22 July 1983)

Zh. Eksp. Teor. Fiz. **86**, 758–773 (February 1984)

The effect of heating of electrons relative to phonons is observed and investigated in a superconducting film that is made resistive by current and by an external magnetic field. The effect is manifested by an increase of the film resistance under the influence of the electromagnetic radiation, and is not selective in the frequency band 10^{10} – 10^{15} Hz. The independence of the effect of frequency under conditions of strong scattering by static defects is attributed to the decisive role of electron-electron collisions in the distribution function. The experimentally obtained characteristic time of resistance variation near the superconducting transition corresponds to the relaxation time of the order parameter, while at lower temperatures and fields it corresponds to the time of the inelastic electron-phonon interaction.

I. INTRODUCTION

The action of low-intensity electromagnetic radiation on a homogeneous superconductor has by now been sufficiently fully investigated.¹ Much less investigated was the action of radiation on the resistive state, which is spatially inhomogeneous and therefore quite complicated. Detailed investigations were made in the latter case only of thermal phenomena connected with heating of the superconductor as a whole relative to the thermostat (bolometric effect). Yet it is of considerable interest to observe nonthermal phenomena due to the action of radiation on a superconductor in the resistive state, when the electron distribution function is nonequilibrium under conditions of good heat dissipation, and the phonons serve as the thermostat. This subject has been only little studied. Stimulation of superconductivity in the resistive state by a microwave field was observed in Ref. 2. In Refs. 3–5 were investigated the suppression of superconductivity by high-intensity laser radiation, whereby the superconductor became resistive; principal attention was paid to measurements of the characteristics of such a transition. In Refs. 3 and 4 was investigated only the critical radiation power needed for a transition to the resistive state. In Ref. 5, in addition, the effect of increasing the radiation power and raising the temperature on the current-voltage characteristics (CVC) were compared, and it was concluded that the action of the radiation is not thermal. However, the limited character of the measurements, particularly the use of a fixed radiation frequency and study of only the stationary state, hinder the understanding of the observed phenomena and makes it impossible to separate them completely from the known thermal effect.

We have investigated in this study the action of low-intensity electromagnetic radiation on a superconducting film in the resistive state. The distinguishing features of the experiment are the use of a wide range of radiation frequencies, from the radio band to the ultraviolet, an investigation of the kinetics of the nonstationary processes with the aid of high-frequency modulation of the radiation, and the use of

various methods to produce the resistive state. The resistive state was produced either by transport current near the critical temperature T_{cr} , or by a current and an external magnetic field at lower temperatures. The investigated objects were narrow (width $W = 1$ – $10 \mu\text{m}$) and thin ($d = 100$ – 500 \AA) Nb films on a sapphire substrate, ensuring good thermal contact with the thermostat. The film resistance R was found to be increased by the radiation independently of the frequency in the band $\nu = 10^{10}$ – 10^{15} Hz. The time delay in this frequency interval remained unchanged at fixed values of the current I , the external magnetic field H , and the temperature T .^{6,7} The resistance increase was demonstrated by a set of experiments to be nonbolometric. The effect was shown to be unconnected with the method of producing the resistive state (phase-slippage centers (PSC) at $T \sim T_{cr}$ and vortices far from T_{cr}). We determined the dependence of the characteristic resistance-change time τ on the temperature and on the magnetic field. The features of the effect made it possible to attribute it to radiative heating of the electron system relative to the phonon system, and to the influence of this heating on the film resistance in the resistive state. The nonselectivity of the action of the radiation in so wide a range of frequencies is explained by the decisive role played by electron-electron collisions in the formation of the distribution function in strong scattering by static defects.⁸ In this case the radiation quantum energy is distributed over the electron subsystem, so that the action of the radiation on the film resistance is determined only by the absorbed power. The measured time constant τ corresponds to the order-parameter relaxation time τ_{Δ} near the superconducting transition and to the inelastic electron-phonon interaction time τ_{eph} at lower values of T and H .

The plan of the article is the following. In the second section we describe the sample-preparation and experimental techniques. Principal attention is paid to a nonstandard procedure for measurements in a very wide frequency band and for the investigation of the kinetics of the processes with resolution up to 10^{-9} sec in the millimeter and submillimeter bands. In the third section we report the main experi-

mental result. Their analysis and a discussion of the nature of the observed are contained in the fourth section and in the conclusion.

II. EXPERIMENTAL PROCEDURE

1. The films were prepared by high-frequency sputtering of 99.9999% pure niobium in an atmosphere of 99.995 pure argon. The vacuum chamber was evacuated beforehand to $(1-2) \times 10^{-6}$ mbar, and the sputtering was carried out without decreasing the evacuation rate at an argon pressure 3×10^{-3} mbar. The films were deposited at a rate of 600 Å/min on optically polished etched beforehand in a high-frequency discharge and then heated to 600 C. The film thickness, determined from the sputtering time, was $d = 100-500$ Å; the film square resistance R_{\square} varied in this case in the range 50–5 Ω. With decreasing niobium film thickness, a decrease of T_{cr} is observed, due to the proximity of the oxygen-rich surface layer to the film.⁹ Decreasing the thickness d of the investigated films obtained under optimal conditions from 500 Å to 100 Å causes T_{cr} to decrease from 8 to 4 K. The superconducting-transition width (between $0.1 R^{10}$ and $0.9 R^{10}$, where R^{10} is the resistance measured at 10 K) did not exceed 0.2 K for such films and was due to the superconducting fluctuations.

Depending on the experimental needs, photolithography and subsequent chemical etching were used to produce samples in the form of narrow strips, either single or bent into fretworks made up of links connected in parallel, series-parallel, or series. The width of the narrow strips, including of the individual links of the fretwork, was $W = 1-10 \mu\text{m}$. The combined length L of the sample strips was varied from 100 μm to 80 cm. Owing to the small film thickness, there was practically no chemical underetching, and electron-microscope investigations have shown that the edge defects of the produced structures were smaller than 500 Å. The sample area S did not exceed 0.2 cm², and the sample resistance in the normal state, depending on the thickness and on the interconnection of the individual links, ranged from 30 to 10^6 Ω.

We determined the following parameters of the investigated samples: critical temperature T_{cr} , electron mean free path l , coherence length $\xi(0)$, effective depth of penetration of the perpendicular magnetic field $\delta_{\perp}(0)$, equilibrium energy gap 2Δ , and coefficient α of absorption of electromagnetic radiation of frequency $\nu \ll \tau_p^{-1}$ (τ_p is the momentum relaxation time) by a normal film having a large area ($S \gg \lambda^2$, where λ is the wavelength). The dc measurements were by the standard four-contact method in the current-generated regime,

with the current-voltage characteristics recorded with a plotter. Homogeneous Ginzburg-Landau pair-breaking currents are realized for all the investigated samples near the superconducting-transition temperature. The value of T_{cr} was obtained by linear extrapolation of the temperature dependence of the critical current $(I_{cr}(T))^{2/3}$ to zero. The critical magnetic field was determined from the midpoint of the resistive transition at a measuring current $10^{-7}-10^{-6}$ A. The coherence length $\xi(0)$, the electron mean free path l , and the depth of penetration of the perpendicular magnetic field $\delta_{\perp}(0)$ were calculated from the experimental data using the known formulas given, e.g., in Ref. 10. The absorption coefficient α of the investigated films was calculated within the framework of the free-electron model.¹¹ The expression for the absorption coefficient at radiation frequencies $\nu \ll \tau_p^{-1}$ and for films of thickness less than the skin-layer depth takes the simpler form

$$\alpha = 4R_{\square}^{10}/R_0(1+2R_{\square}^{10}/R_0)^2, \quad (1)$$

where R_{\square}^{10} is the film square resistance measured at 10 K, and $R_0 = 377 \Omega$ is the wave resistance of free space. In this case α is a parameter that does not depend on the radiation frequency. The decrease of the absorption coefficients at frequencies $\nu > \tau_p^{-1}$ is described by the factor $[1 + (2\pi\nu\tau_p)^2]^{-1/2}$. The values of α for the investigated films ranged from 0.05 to 0.3.

To check on the calculated values of α , we measured the transmission coefficient Π of a normal film in several transparency regions of the sapphire substrate (e.g., $\lambda = 2-0.2$ mm, $\lambda = 3-5 \mu\text{m}$, and others) and compared with the calculated $\Pi = (1 + R_0/2R_{\square}^{10})^{-2}$. The agreement, within 30% or less, between the calculated and experimental transmission coefficients attests to the reliability of the calculated values of α .

The equilibrium energy gap 2Δ was determined by measuring the transmission spectrum of a large-area whole film at millimeter and submillimeter wavelengths ($\lambda = 8-0.2$ mm). The measurement procedure is described in Ref. 12.

The effective thermal conductivity G needed to assess the role of the thermal phenomena and describing the heat transfer from the electrons to the phonons in the case of electron heating, or through the boundary between the film and the thermostat, was calculated in the case of the bolometric effect from the measured hysteresis of the critical currents¹³:

$$G = 4AT^3, \quad (2a)$$

where

TABLE I. Sample parameters.

N°	$d, \text{Å}$	$w, \mu\text{m}$	L, mm	T_{cr}, K	$R_{\square}^{300}, \Omega$	R_{\square}^{10}, Ω	$l, \text{Å}$	$\xi(0), \text{Å}$	$\frac{D}{\text{cm}^2 \cdot \text{c}^{-1}}$	Type*	$\rho^{10} \cdot 10^5, \Omega \cdot \text{cm}$	$v_F \cdot 10^8, \text{cm} \cdot \text{c}^{-1}$	$\delta_{\perp}(0), \mu\text{m}$
1	120	2,0	0,3	3.92	28	22.8	5	57÷70	0.7	A	2.73	4	4.8
2	200	1,3	5,8	3.94	21	17	6	62÷86	1.0	B	3,4	5	3.6
3	180	1,2	0,1	6.2	24,6	16.4	12	73÷58	0.73	A	2,9	1.7	2.2
4	210	2,0	5,8	6.5	20,7	13.8	13	71÷90	1.8	B	2,9	4,2	1.8
5	100	2,2	0,3	3,3	50,7	42,4	5.1	62	0.68	A	4,2	4	10.7

*A—individual strip, B—fretwork; ρ^{10} —resistivity of sample at $T = 10$ K; v_F —Fermi velocity.

$$A = I_{cr2}^2 R^{10} / W L d (T_1^4 - T^4). \quad (2b)$$

Expression (2b) was obtained under the assumption that the current I_{cr2} (the current at which the sample goes over from the normal to the superconducting state) is the critical current at a temperature T_1 higher than the helium-bath temperature T . The value of T_1 was obtained from the relation

$$I_{cr}(t) = 0.25 I_{cr}(0) (1 + t^2)^{3/2} (1 - t^2)^{1/4},$$

where $t = T / T_{cr}$ and $I_{cr}(0)$ was determined from measurements of $I_{cr}(T)$ near T_{cr} .

The parameters of several typical samples are listed in Table I.

2. To shed light on the mechanism of the observed effect and to reveal it against the background of the previously known ones, a number of experimental programs must be executed. These include an investigation of the action of radiation in various bands (from radio to ultraviolet), measurement of the characteristic relaxation times, study of the thermophysical characteristics to reveal the role of thermal effects, and others. A single experimental setup is therefore ineffective. For the sake of clarity, Fig. 1 shows a generalized block diagram in which dashed outlines surround blocks of like purpose. Electromagnetic radiation from the source (S) passes through a modulator (M), through a setup for filtering or measuring the wavelengths (F), and also through a matching coupling element (C), and enters a quasi-optical waveguide (WG) located in a crystate and guiding the radiation to the sample (Smp). The sample is connected either to a dc measurement system (DC) or to a high-frequency recording system (HF).

The radiation sources are klystrons (K) in the centimeter and millimeter bands, backward-wave tubes (BWT) in

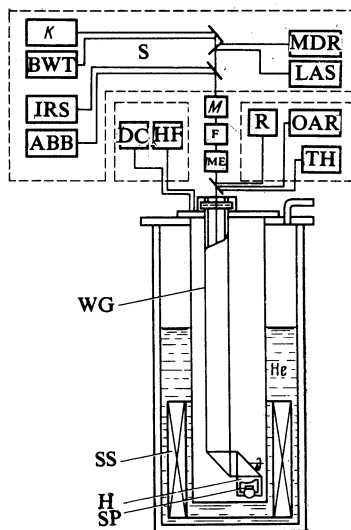


FIG. 1. Schematic block diagram of experimental setup. S—radiation-source block: K—klystrons, BWT—backward-wave tubes, ABB—absolutely black body, MDR—monochromator, LAS—laser, R—radiometer, OAR—opto-acoustic receiver, TH—thermistor head, DC—dc recording system, HF—hf recording system, M—modulator, F—apparatus for filtering the radiation and measuring the wavelength, ME—matching element, WG—quasi-optical waveguide, H—sample holder, Sp—sample, SS—superconducting solenoid.

the submillimeter band, IR spectrometers (IRS) and an absolutely black body (ABB) with a set of filters in the infrared, and lasers (LAS) and a mercury-lamp monochromator (MDR) in the visible and ultraviolet (UV). The radiation power was measured with thermistor heads (TH) in the microwave bands, an opto-acoustic receiver (OAR) in the submillimeter band, and a radiometer (R) in the infrared, optical and UV bands.

A sample holder (H) with three degrees of freedom permits smooth adjustment and exact orientation of the sample plane parallel and perpendicular to the external magnetic field. A channel with the holder on which a heater and a germanium thermometer are mounted is placed either in a vacuum jacket or directly in liquid helium. The magnetic field is produced by a superconducting solenoid (SS). The action of the magnetic radiation is revealed by the change of the sample resistance, i.e., by the increase of the voltage ΔU on the resistor at fixed values of I , H , and T . The value of ΔU is measured as a rule at the frequency of the amplitude modulation of the radiation. ΔU is measured with a standard synchronous detector circuit and recorded on a plotter as a function of I , H , and T . Under the same experimental conditions we measured the slope dU/dT of the sample voltage. To this end, the temperature was changed by a fixed amount $\Delta T = 10^{-3} - 10^{-4}$ K with a heater or by changing the helium vapor pressure, and the value of $\Delta U_T = (dU/dT)\Delta T$ recorded.

3. When spectral investigations are made in a wide frequency band $\nu = 10^{10} - 10^{15}$ the main difficulty lies in maintaining constant the radiation power incident on the investigated sample. The capabilities of incoherent radiation sources for this band are limited, while the use of coherent radiation sources raises difficulties connected with interference of the radiation in the channel and in the receiving head with the investigated sample. The latter difficulty can be avoided by obtaining a uniform radiation-power distribution over the channel cross section. This is done by using a quasi-optical procedure in a multimode regime, even when working with radiation whose wavelength is comparable with the transverse dimensions of the channel. In this case the radiation power incident on the sample can be calculated from measurements of the total power in the channel cross section.

From technical considerations, the spectral range covered in the experiment is traditionally divided into four regions—microwave, submillimeter, infrared, and optical. Each uses its own methods of channeling the radiation and measuring its power. In the present study we used in all four regions of the spectrum a quasi-optical channel in the form of an internally polished stainless steel tube of 20 or 40 mm diameter (the latter was used in the wavelength interval $\lambda = 4 - 0.8$ cm). The radiation power was made uniform over the tube cross section by using at its input a beam spreader for the proper band (horn for microwaves, cone for millimeter and submillimeter waves, and a system of quartz lenses for optical and ultraviolet radiation).

The quasi-optical scheme was verified independently in the microwave and infrared bands. In the former case a coaxial technique was used, permitting an exact measurement of

the high-frequency power absorbed in the sample. In the second case we used for the same purpose an absolutely black body and a hollow dielectric waveguide with absorbing walls. The integral radiation power incident on the sample can be directly calculated from geometric considerations. In both cases the spectral characteristics and the magnitude of the investigated effect turned out to differ from those obtained with the quasi-optical measurement procedure by not more than a factor of two.

When investigating the spectral characteristic of the heating of electrons in the nonresistive state of a superconducting film it is necessary in principle to take into account the frequency dependence of its absorption coefficient; this dependence is connected both with the diffraction of the radiation by the sample structure and with the specific features of the resistive state. Allowance for the first of these factors is in the general case quite complicated. Therefore the samples used for the spectral investigations were in the form of fretworks with large filling coefficient, for which estimates have shown that the absorption coefficient in the frequency interval $\nu = 10^{10} - 10^{15}$ Hz differs from that calculated from (1) by not more than a factor of two. The calculation of α for a film in a homogeneous superconducting state, in the entire range of magnetic fields and temperatures used in the experiments, indicates that the values of change in this interval by less than a factor of two. In the resistive state the spectral dependence of the absorption coefficient can obviously only become weaker. Thus, the possible frequency dependence of α lies within the limits of the accuracy of our spectral measurements, so that under the experimental conditions we can use for the investigated samples the absorption coefficient calculated for a normal film.

4. The time constant of the effect was measured directly by high-frequency modulation of the millimeter and submillimeter waves¹⁴ and by pulsed modulation for the near ultraviolet. High-frequency amplitude modulation of the BWT radiation ($\lambda = 0.2 - 8$ mm) was produced by two methods. In the first (Fig. 2a) a resistor was connected in the anode circuit of the plate and voltage from an HF generator was applied to it from a decoupling capacitor; the resultant depth of modulation of the anode voltage U_a was about 0.1%. By choosing the operating point of the BWT on the slope of the genera-

tion band, it is possible to obtain, besides the frequency modulation that is inessential in this case, the required amplitude modulation with depth up to 100%. However, synchronous noise at the HF generator frequency interferes with the measurements. It is therefore convenient to include an interferometer in the quasi-optical channel. This permits the operating point of the BWT to be shifted, by the same HF generator voltage, by several interference fringes. The amplitude modulation frequency is in this case $f = 2nF$, where F is the frequency of the HF generator and n is the number of employed interference fringes. In the experiment we chose usually $n = 5 - 10$; the maximum values of f were then $\sim 10^8$ Hz. A radiation modulation depth close to 100% was achieved by proper choice of the ray path difference and of the transmission coefficient of the beam splitting plate (BS) of the interferometer. The second method (Fig. 2b), which can yield a modulation frequency $f = 10^6 - 10^9$ Hz, consists of using the oscillation beats of two BWT operating at close frequencies. Two identical tubes are connected to a common anode-voltage source, and their output guided into one channel with a beam splitter. In the anode circuit of one of the tube is connected a resistor to which is applied from an external source a bias voltage that determines the difference between the tube frequencies, and hence the beat frequency. The radiation power of the tunable-frequency BWT is maintained constant with an attenuator (AT), thereby reaching a constant modulation depth. The values of τ were determined also in the UV band, using for this purpose an N_2 laser with pulse duration 10 nsec. At high modulation frequencies the voltage ΔU was picked off through a coaxial cable; the $\Delta U(f)$ dependence was recorded with a spectrum analyzer, and the signal pulse waveform with a stroboscopic oscilloscope. The sample was shunted in this case to match it to the recording system.

III. EXPERIMENTAL RESULTS

As already noted, an exhaustive investigation of the effect called for the use of samples with a variety of geometries. To facilitate the comparison of the experimental data we present below where possible the results for one typical sample, No. 1 (see the table). The only exceptions are cases when the parameters of the samples were varied or when the indicated sample was not optimal for the specific experiment.

The current-voltage characteristics (CVC) of sample No. 1, measured at $T \sim T_{cr}$ and $H = 0$, are shown in Fig. 3. The parameter of the set of curves is the temperature. The figure shows also for the same CVC the current dependences of $\Delta U(I)$ obtained when the radiation applied to the sample had an intensity low enough to be able to use the linear section of the $\Delta U(P)$ plot (P is the radiation power incident on the sample). The maximum value of $\Delta U(I)$ increases with decreasing temperature in the interval $0.9 < t < 1$. At lower temperatures, in the absence of a magnetic field, the CVC become discontinuous and hysteresis of the critical current appears. Continuous CVC can be obtained in this case by introducing a magnetic field (Fig. 4), but the functions $\Delta U(I)$ and $U(I)$ remain qualitatively the same as at $H = 0$ near T_{cr} . We note that the forms of these functions and the character-

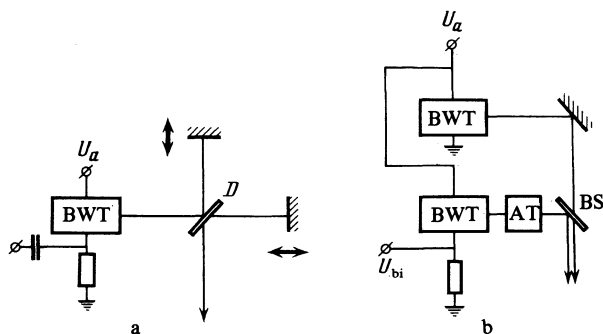


FIG. 2. High-frequency modulation schemes for BWT radiation: a— with interferometer in channel and modulation of BWT anode voltage U_a ; b— using beats of two BWT of close frequency, AT—attenuator, U_{bi} —bias voltage, BS—beam-splitting plate.

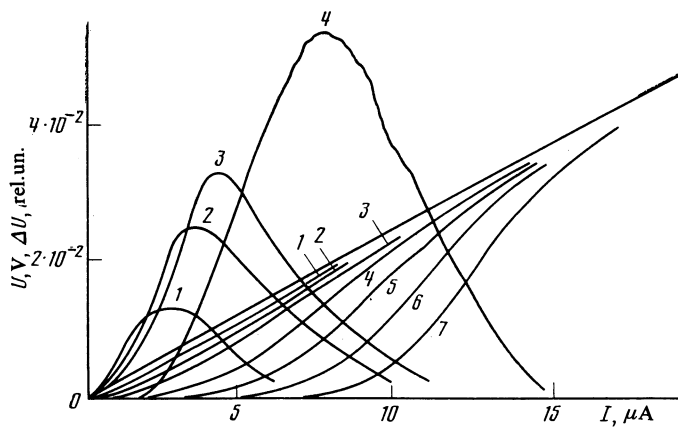


FIG. 3. Current-voltage characteristics (1-7) and plots of $\Delta U(I)$ (1'-4') for sample No. 1. $H = 0$, $\nu = 300$ Hz. Values of t : 1, 1'—0.999; 2, 2'—0.998; 3, 3'—0.995; 4, 4'—0.989; 5—0.987, 6—0.985, 7—0.982.

istic values of the current do not change when the orientation of the magnetic field changes from perpendicular to the film plane (H_{\perp}) to parallel (H_{\parallel}) provided the field $h = H/H_{cr}(T)$ referred to the critical value at the given temperature remains constant. The ratio $H_{cr\parallel}/H_{cr\perp}$ of the critical magnetic fields at a fixed temperature $T \ll T_{cr}$ depends substantially on the film thickness and ranges from 1.2 to 4 when the film thickness is decreased from 500 to 120 Å. At low temperatures ($t < 0.9$) the presence of the magnetic field causes ΔU to depend already on three quantities, I , H , and T . If the power P of the radiation incident on the sample is fixed, the two-parameter function $\Delta U(I, H)$ has an absolute maximum that shifts into the region of stronger magnetic fields and smaller currents with decreasing temperature. This is illustrated in Fig. 5, where plots of $\Delta U(I, H)$ are shown for sample No. 4 at two different temperatures and at constant P .

Figure 6 shows the dependence of $\Delta U/L$, normalized to the sample length, on the width W at a constant film thickness ($d = 120$ Å). The measurements were performed at identical values of h and t ($h = 0.9$, $t = 0.7$) and at fixed radiation flux density. The current for each sample was chosen to correspond to the maximum of $\Delta U(I)$. Attention is called to the steep growth of the effect at $W < 10$ μm.

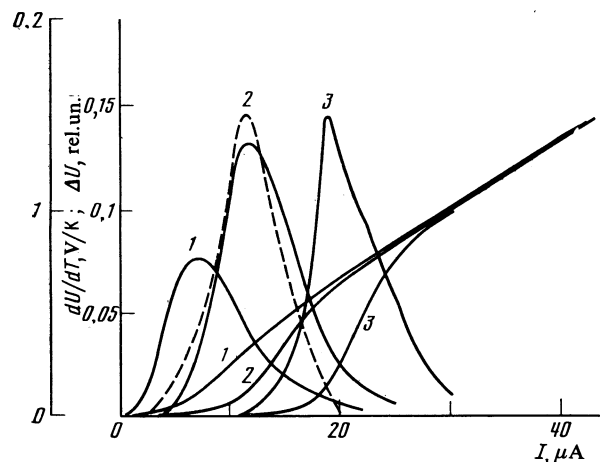


FIG. 4. Current-voltage characteristics (1-3) and plots of $\Delta U(I)$ (1'-3') and $dU/dT(I)$ (dashed) in a magnetic field for sample No. 1 (magnetic field perpendicular to plane of film), $t = 0.5$, $\nu = 300$ Hz, H (kOe): 1, 1'—22.3; 2, 2'—20.6; 3, 3'—18.6.

To measure the dependence of ΔU on the radiation frequency ν it is convenient to use a sample in the form of fretwork with a large filling coefficient. Notice should be taken of the experimentally observed constancy of ΔU in a very wide frequency interval, $\nu = 10^{10}$ – 10^{14} Hz, at a fixed incident power on the film (the fall-off of ΔU at $\nu \gg 3 \times 10^{14}$ Hz can be attributed, as shown by calculation, to the change of the absorption constant α at these frequencies). When T , I , and H are varied, only the absolute value of ΔU changes, while the spectral characteristic of the effect remains unchanged. A plot of $\Delta U(\nu)$ for sample No. 2 is shown in Fig. 1 of Ref. 7.

The typical amplitude-frequency characteristic from which the time constant of the effect can be determined is uniform up to the frequency f_0 , and with further increase of the amplitude-modulation frequency f the value of ΔU decreases. A typical $\Delta U(f)$ dependence is shown in Fig. 2 of Ref. 7 (curve 1). This dependence is well described by the expression

$$\Delta U(f) = \Delta U(0) [1 + (f/f_0)^2]^{-1/2}. \quad (3)$$

We can therefore introduce for the effect a time constant $\tau = (2\pi f_0)^{-1}$ whose temperature dependence for samples 1 and 3 is shown in Fig. 7. With decreasing temperature the values of τ go through a minimum, after which they increase in proportion to T^{-2} . The abrupt increase of the time constant near T_{cr} is described by the expression $\tau \sim (1 - t)^{-1/2}$.

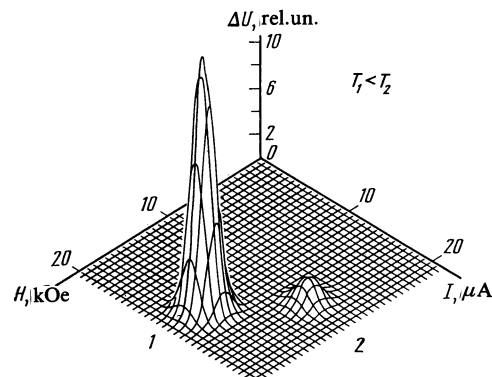


FIG. 5. Plots of $\Delta U(I, H)$ for sample No. 4 at two different temperatures: 1— $t = 0.25$; 2— $t = 0.65$.

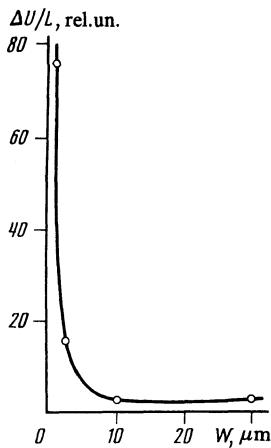


FIG. 6. Plot of $\Delta U/L$ vs sample length. $d = 120 \text{ \AA}$, $t = 0.7$, $h = 0.9$.

At a fixed temperature in the region $t < 0.8$ the values of τ do not depend on the current, nor on the magnetic field up to $H \approx 0.9H_{cr}(T)$, while in stronger fields τ decreases slowly (inset of Fig. 7). With increasing sample width the $\tau(T, H)$ dependence becomes weaker.

Additional measurements were needed to distinguish the investigated effect from the bolometric one. The dependences of ΔU and of the slope dU/dT on the current through the sample is shown in Fig. 4; it can be seen that they have practically the same shape and the same position of the maximum. The plots of $\Delta U(H)$ and dU/dT vs H , measured at fixed T and I , are also close in shape. However, the temperature dependences of ΔU and dU/dT obtained under identical conditions differ substantially (Figs. 8 and 9). The plots shown in Fig. 8 were measured at the absolute maximum of $\Delta U(I, H)$, and those on Fig. 9 at a fixed current $I \ll I_m$ (I_m is the current corresponding to the absolute minimum of $\Delta U(I, H)$). In the latter case the magnetic field was adjusted with changing temperature in such a way that the sample resistance remained constant.

Besides the $\Delta U(f)$ dependence for samples sputtered on sapphire substrates, we measured the analogous dependence for like samples but sputtered on glass. In this experiment the samples were not immersed in liquid helium, so that the heat transfer was through the substrate. The experimental

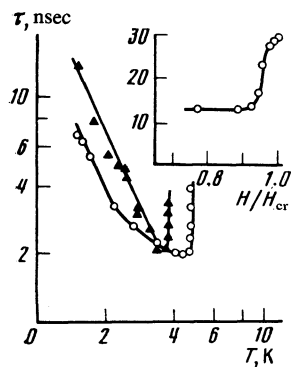


FIG. 7. Temperature dependence of $\tau(I = 5 \mu\text{A})$: \blacktriangle —sample No. 1, \circ —sample No. 3. Inset—dependence of τ on the magnetic field for sample No. 1, $t = 0.4$.

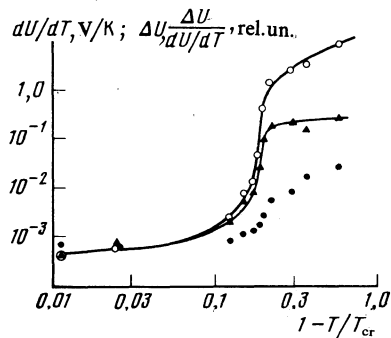


FIG. 8. Temperature dependences of ΔU and dU/d for sample No. 1, measured in the regime of absolute maxima of the current and of the magnetic field: \circ — ΔU , \blacktriangle — dU/dT , \bullet — $\Delta U(dU/dT)^{-1}$.

value of the thermal conductivity G for a sample on a sapphire substrate is larger by more than an order of magnitude than G for a glass sample. An example of the $\Delta U(f)$ dependence for samples sputtered on sapphire and glass is shown in Fig. 2 of Ref. 7 (curves 1 and 2, respectively). At low modulation frequencies, for a film on glass, ΔU decreases with increasing frequency, whereas at high modulation frequencies curves 1 and 2 coincide. We note with increasing thickness of films on sapphire, $\Delta U(f)$ shows a decrease similar to that observed for a thin film on glass. In addition, at low modulation frequency, for relatively thick sapphire-substrate films ($d > 300 \text{ \AA}$) immersed in liquid helium, the value of ΔU becomes discontinuous on going through the λ point, but there is no discontinuity for thin films.

IV. DISCUSSION OF RESULTS

1. Among the known mechanisms whereby radiation acts on a superconductor in a resistive state, only the bolometric effect is independent of frequency in a very wide range. Therefore before proceeding to a discussion of the observed effect, we must stop to analyze the experimental data

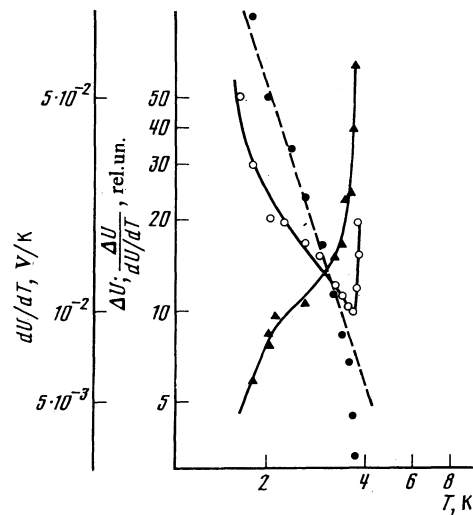


FIG. 9. Plots of $\Delta U(T)$ and $dU/dT(T)$ for sample No. 1. $I = 1 \mu\text{A}$, $R = 0.4R^{10}$. \circ — ΔU , \blacktriangle — dU/dT , \bullet — $\Delta U(dU/dT)^{-1}$, the dashed curve shows a plot of T^{-3} .

that prove its nonthermal origin, and the experimental data needed to distinguish the investigated phenomenon from the thermal effects.

We consider first the functions $\Delta U(I)$, $\Delta U(\nu)$, and $\Delta U(f)$, which might seemingly be explained within the framework of a superconducting film bolometer. Actually, the function $\Delta U(f)$ given by Eq. (1) is applicable for a lumped-parameter bolometer¹⁵ whose response is

$$\Delta U = \frac{\alpha P dU/dT}{WGL} \frac{1}{[1 + (2\pi f \tau_b)^2]^{1/2}}. \quad (4)$$

Here the bolometer time constant is

$$\tau_b = dc_0/G, \quad (5)$$

where c_0 is the specific heat of the film. Expression (4) explains qualitatively the agreement between the dependences of $\Delta U(\nu)$ and $\alpha(\nu)$, dU/dT on I and $\Delta U(I)$, of dU/dT on H and $\Delta U(H)$, as well as the fact that the frequency characteristic $\Delta U(f)$ is uniform up to a frequency f_0 identified in this case with $(2\pi\tau_b)^{-1}$. However, a quantitative analysis of the results contradicts the bolometer model, viz., the experimentally obtained values of ΔU and $\tau = (2\pi f_0)^{-1}$ differ substantially from those calculated from Eqs. (4) and (5). Thus, for sample No. 2, in the form of fretwork filling a square with side $a = 150 \mu\text{m}$, the action of ABB radiation ($T = 500 \text{ K}$, $\lambda_{\text{max}} \ll a$) at a power $P = 2 \times 10^{-10} \text{ W}$ leads to a value $4 \times 10^{-5} \text{ W}$. In the experiment the sample was immersed in superfluid helium ($T = 2.0 \text{ K}$), so that to estimate ΔU_b we must use the published value of the thermal conductivity G of the interface between the film and the helium. At this temperature its value is approximately¹⁶ $5 \text{ W} \cdot \text{cm}^{-2} \cdot \text{K}^{-1}$. Using the experimental value $dU/dT = 2 \text{ V/K}$ and assuming α to be equal to 0.15 [see (1)], we obtain $U_b = 2 \times 10^{-7} \text{ V}$. When estimating τ it must be borne in mind that at low temperatures the lattice specific heat is low compared with the electronic $c_e = \gamma T$, where γ is determined from the experimental values of the resistivity ρ^{10} and the diffusion coefficient D by means of the formula $\gamma = \pi^2 k^2 / 3e^2 D \rho^{10}$, and amounts to $7.0 \times 10^{-4} \text{ J} \cdot \text{cm}^{-3} \cdot \text{K}^{-2}$ for the sample in question, a value close to γ for bulky niobium¹⁷ ($7.2 \times 10^{-4} \text{ J} \cdot \text{cm}^{-3} \cdot \text{K}^{-2}$). At $T = 2.0$ we obtain from (5) $\tau_b = 6 \times 10^{-10} \text{ sec}$, which differs substantially from the experimental value 4×10^{-9} at the same temperature (Fig. 7).

Qualitative discrepancies with the bolometer model can also be indicated. Examples are the temperature dependences of τ and ΔU . The experimentally observed $\tau(T)$ curve has nothing in common with (5); thus, the observed rapid growth of τ at $T \sim T_{\text{cr}}$ is a property of only times typical of the superconducting state, such as the relaxation times of the modulus and phase of the order parameter. The temperature dependence of ΔU (Fig. 9) also differs substantially from that expected for a bolometer

$$\Delta U_b \sim \frac{dU}{dT}(T)/G(T).$$

In particular, the jump of the thermal conductivity G on going through the λ point of liquid helium does not affect the $\Delta U(T)$ dependence.

In addition, we performed a special experiment to com-

pare bolometric and investigated effects. The bolometric effect can be observed, for example, by decreasing the heat removal from the film: for a film on a glass substrate it manifests itself at $f < 10^5 \text{ Hz}$ (Fig. 2c of Ref. 7, curve 2). The decrease of ΔU with frequency, observed here and described by the relation $\Delta U \sim f^{-p}$ ($0.5 < p < 1$), is typical of a bolometer with distributed parameters.¹⁸ At high modulation frequencies the bolometric effect ceases to manifest itself, and the characteristics of the investigated effect do not depend on G and are the same for both samples.

Thus, although in a number of manifestations the effect investigated is similar to the bolometric one, the aggregate of the results proves it to be of nonthermal origin. The bolometric effect can predominate under certain conditions at low radiation-modulation frequencies. With increasing modulation frequency, however, the effect reported here becomes dominant.

We must stop now to discuss the choice of the geometry of the samples (of sufficiently thin and narrow films) needed to optimize the conditions for observing the investigated effect and suppressing the bolometric one. Nonthermal action of radiation predominates if in the film the phonon lifetime, limited by the inelastic scattering from electrons (τ_{phe}), is much shorter than the phonon escape time (τ_{es}) from the film. Clearly, to decrease its heating the film must be thin enough, since τ_{es} is proportional to the thickness d and the value of τ_{phe} , which coincides near the superconducting transition $\Delta(T, H)/kT \ll 1$ with the corresponding time in a normal metal, is practically independent of d .¹⁹ Additional increase of the heat removal from the investigated film can be obtained by using a sufficiently narrow strip,²⁰ whereby a decrease of the return flow of nonequilibrium phonons from the substrate is decreased. In addition, a decrease in the film width causes an increase of the investigated effect (Fig. 6), while a decrease of the thickness leads to an increase of the absorption coefficient [see (1)].

2. Having established the nonthermal nature of the observed effect, we can propose that it is connected with electron heating by the applied radiation. Let us analyze from this point of view the main distinguishing features of the effect—its independence of the radiation frequency, the characteristic temperature dependence of the time constant, and a number of others.

The nonselectivity of the effect seems at first glance unexpected, since the electron-phonon energy-relaxation mechanism, discussed until recently in connection with the homogeneous superconducting state, leads to a substantial dependence of the distribution function and of the order parameter on the radiation frequency.²¹ The electron-electron collisions that lead to a redistribution of the energy of the radiation quantum over the electron subsystem, is neglected here. The justification of such an approach in the case of pure superconductors is the relatively low effectiveness of inelastic electron-electron interaction, both at $T \sim T_{\text{cr}}$ for superconductors with $T_{\text{cr}} > 1 \text{ K}$, and in the region of low temperatures (without a magnetic field) because of the low quasiparticle density.

In the case of interest to us, of strong scattering by static defects, the electron-electron interaction becomes stronger,

as shown in Ref. 8, so that the corresponding energy relaxation time τ_{ee} is shortened. In particular, under the condition $d \lesssim (\hbar D / kT)^{1/2}$ (D is the diffusion coefficient), which is realized in experiment, we have

$$\tau_{ee} = \frac{\hbar}{kT} \frac{2\pi^2 \hbar}{e^2 R_{\square}^{10}} \ln^{-1} \frac{\pi \hbar}{e^2 R_{\square}^{10}}. \quad (6)$$

For films with $R_{\square}^{10} = 40 \Omega$ an estimate according to (6) yields $\tau_{ee} = 2 \times 10^{-10}$ sec at $T = 10$ K. Comparison of the energy relaxation times τ_{ee} and τ_{eph} obtained for the investigated films in an experimental investigation of the quantum corrections to the conductivity,²² shows that in films ~ 100 Å thick, for quasiparticles of energy $\varepsilon \ll kT_0$ ($T_0 = 10$ K), the electron-electron interaction is indeed more effective than the electron-phonon one. In a substantial energy region $\varepsilon \sim kT$ it is therefore precisely the electron-electron collisions that govern the excitation distribution function f_{ε} — the Fermi function with temperature $\Theta \neq T$ and with zero chemical potential. At high energies, where the energy relaxation is via inelastic electron-phonon collisions, the high-energy phonons emitted by the quasiparticles are reabsorbed and do not leave the film, whereas for the thermal phonons the film is transparent. Thus the entire absorbed radiation energy enters in the energy region $\varepsilon \sim kT$ and is redistributed in the electron subsystem via electron-electron collisions. The investigated effect is therefore nonselective in a wide frequency range, including both high phonon energies (T_D , the Debye temperature) and low ones (kT).

For further discussion it is convenient to divide the temperature interval into two regions, near T_{cr} ($\Delta / kT \ll 1$) and a lower-temperature region ($\Delta / kT \sim 1$).

Near the critical temperature the situation is apparently isothermal (spatially-homogeneous heating), since at $\Delta / kT \ll 1$ the resistive state is connected with formation of phase-slippage centers (PSC).²³ The form the CVC in this case is determined by large static regions between the PSC, of size on the order of $l_E = (4TD\tau_{ee}/\pi\Delta)^{1/2}$ (l_E is the penetration depth of the longitudinal electric field E). The action of the radiation leads to suppression of the order parameter in the region between the PSC and to an increase of l_E . In the case of an isothermal resistive state the action of the electromagnetic field can be described by the electron bolometer model, $\Delta U = (dU/d\Theta)\Delta\Theta$, where $\Delta\Theta$ is determined from the balance equation

$$c_e \dot{\Theta} = G_e (\Theta - T) + P_0. \quad (7)$$

Here P_0 is the total power released per unit volume,

$$c_e = \int \frac{\partial(\varepsilon f_{\varepsilon})}{\partial \Theta} N_{\varepsilon} d\varepsilon$$

(N_{ε} is the density of states), and the term $G_e (\Theta - T)$ describes the heat transfer from the electrons to the phonons. Inasmuch as the quasiparticle scattering and recombination times near the superconducting transition are of the order of the time τ_{eph} of the energy relaxation in a normal metal, we have apart from a coefficient of order unity

$$G_e = \int \tau_{eph}(\varepsilon)^{-1} \frac{\partial(\varepsilon f_{\varepsilon})}{\partial \Theta} N_{\varepsilon} d\varepsilon \equiv c_e / \tau_{ee}.$$

The averaged time τ_e of the energy relaxation of the electron subsystem coincides in the lower-temperature region with the measured time constant τ of the effect. Assuming that $dU/d\Theta = dU/dT$ and extrapolating (T) into the region of the superconducting transition, we find that the value of the effect calculated in accordance with (7)

$$\Delta U = \frac{\alpha P \tau dU/dT}{LWdc_e} \quad (8)$$

agrees with the experimentally determined values of ΔU . The time constant of the effect in this temperature region does not coincide with the time τ_{eph} , but is determined by the order-parameter relaxation time τ_{Δ} , which is much longer than τ_{eph} at $\Delta / kR \ll 1$. Near T_{cr} the values of τ_{Δ} diverge, $\tau_{\Delta} \approx (kT/\Delta) \tau_{eph} \sim (1-t)^{-1/2}$, as is indeed observed in experiment (Fig. 7). In the case when the proximity to the superconducting transition ($\Delta / kT \ll 1$) is reached on account of the magnetic field, τ is also determined by the order-parameter relaxation time τ_{Δ} . In strong enough fields ($\Gamma/\Delta \gg 1$ but $\Gamma/\Delta < \Delta\tau_{eph}$, where $\Gamma = DeH/c$), τ increases slowly and reaches a value²⁴ $\tau_{\Delta} = \tau_{eph} kT/\Gamma$, in qualitative agreement with the results of Fig. 7.

Of greatest interest is the region of lower temperatures ($\Delta / kT \sim 1$), in which the resistive state has been less investigated. Under the experimental conditions it is produced by a magnetic field and by transport current. The normal regions do not propagate over the entire sample, even though heat is released in them, say due to the presence of inhomogeneities in the sample or through thermoelectric effects.²⁵ When the magnetic field is turned on, these inhomogeneities may be flux vortices. Their viscous motion can also participate in the production of resistance. Experiment shows, however, that all the characteristics of the investigated effect remain the same as before when the orientation of the magnetic field is changed from perpendicular to horizontal relative to the film surface, if the value of H referred to the critical value is preserved. The magnetic flux that pierces the film changes then by more than two orders, so that the investigated effect is not connected with the method by which the resistive state is produced, and its cause cannot be the change of the vortex motion induced by the radiation. Thus, the magnetic field serves only to suppress the order parameter and to decrease the values of the current corresponding to the resistive section of the CVC. The inertia of the effect, which is connected in this temperature region with the electron heating, should be determined by the rate of energy transfer from the electrons to the phonons. The $\tau(T)$ temperature dependence observed in this temperature region ($t < 0.9$), as seen from Fig. 7, is close in form to $\tau \sim T^{-2}$. A similar temperature dependence and close values of the energy-relaxation time were observed in experiments on the effects of weak localization in metallic films of thickness $d \sim 100$ Å (Ref. 22), including direct observation for a number of samples used in the present study.

The foregoing discussion explains in general outline a number of features of the effect on the basis of the very simple model of spatially homogeneous heating of the electrons by radiation. At low temperatures, however, the effect itself, especially for narrow films, does not agree with the calcula-

tion performed in this model. Indeed, when account is taken of the current-source power released in the sample, the maximum value of ΔU is bounded by the condition $I(dU/dT)(\tau/c_e) < 1$ of thermal stability of the CVC,¹⁵ and cannot exceed the value $\Delta U_{\max} = \alpha P/I$ (satisfaction of the cited inequality was verified experimentally by measuring ΔU and dU/dT as functions of the internal resistance of the current source). At the same time, the experimental value of ΔU for sample No. 2 exceeds U_{\max} by an order of magnitude. Nonetheless, the temperature dependence of the effect at low T can be explained by the simplest heating model (Fig. 9). As T_{cr} is approached the ratio of ΔU and dU/dT decreases abruptly (Fig. 8) and at $\Delta/kT \ll 1$ it agrees with the calculation by Eq. (8). The quantity $\tau/c_e = G_e^{-1}$ is determined independently from the hysteresis of the critical currents (2) and for films on sapphire it turns out to be close to that calculated from measurements of τ .

V. CONCLUSION

Observation of the nonselective effect of radiation-induced electron heating in the resistive state of a superconductor was made possible by the specific conditions of the experiment. The electrons become hotter than the phonons if the heat removal from the investigated film is good; this was achieved both by choosing the sample geometry (narrow and thin films), and by modulating the radiation at high frequency. The nonselectivity of the effect is ensured by the substantial role of the electron-electron collisions in the formation of the distribution function when films with small mean free paths are used. To study the weak action of the radiation (the effect linear in the intensity), the resistive state is produced by a transport current and by a magnetic field. If the foregoing conditions are satisfied, the investigated effect manifests itself, as shown by preliminary experiments, also in films of other superconductors, particularly Al and NbN.

We note that in our opinion interest attaches not only to the investigated effect itself, but also to its use to measure the characteristic times τ_{Δ} and τ_{eph} .

- ¹J. A. Pals, K. Weiss, P. M. T. M. van Attekum, R. E. Horstman, and J. Wolter, Phys. Rep. **89**, 323 (1982). V. M. Dmitriev and E. V. Khristenko, Fiz. Nizk. Temp. **4**, 821 (1978) [Sov. J. Low Temp. Phys. **4**, 387 (1978)].
- ²V. M. Dmitriev and E. V. Khristenko, Pis'ma Zh. Eksp. Teor. Fiz. **29**, 758 (1979) [JETP Lett. **29**, 697 (1979)].
- ³L. R. Testardi, Phys. Rev. B **4**, 2189 (1971).
- ⁴A. I. Golovashkin, K. V. Mitssek, and G. P. Motulevich, Zh. Eksp. Teor. Fiz. **68**, 1408 (1975) [Sov. Phys. JETP **41**, 701 (1975)].
- ⁵L. N. Smith, J. Low Temp. Phys. **38**, 553 (1980).
- ⁶E. M. Gershenzon, M. E. Gershenzon, G. N. Gol'tsman, et al., Pis'ma Zh. Eksp. Teor. Fiz. **34**, 328 (1981) [JETP Lett. **34**, 268 (1981)].
- ⁷E. M. Gershenzon, M. E. Gershenzon, G. N. Gol'tsman, et al., *ibid.* **36**, 241 (1982) [36, 296 (1982)].
- ⁸B. L. Al'tshuler and A. G. Aronov, *ibid.* **30**, 514 (1979) [30, 482 (1979)].
- ⁹M. E. Gershenzon and V. P. Koshelets, Zh. Tekh. Fiz. **50**, 572 (1980) [Sov. Phys. Tech. Phys. **25**, 343 (1980)].
- ¹⁰M. Tinkham, Introduction to Superconductivity (Russ. Transl.), Mir, 1982.
- ¹¹M. Born and E. Wolf, Principles of Optics, Pergamon, 1973 (Russ. Transl. of earlier edition, Nauka, 1970, p. 687).
- ¹²E. M. Gershenzon, G. N. Gol'tsman, and A. D. Semenov, Prib. Tekh. Eksp. No. 4 (1983).
- ¹³G. Dharmadurai, Phys. Stat. Sol. (a) **62**, 11 (1980).
- ¹⁴E. M. Gershenzon, G. N. Gol'tsman, and A. D. Semenov, Proc. 3rd All-Union Symp. on Millimeter and Submillimeter Waves, Gorky, Vol. 1, 1980, p. 233.
- ¹⁵K. Rose, IEEE Transactions on Electron Devices ED-27, 118 (1980).
- ¹⁶A. F. G. Wyatt, in: Nonequilibrium Superconductivity, Phonons, and Kapitza Boundaries, K. E. Gray, ed., Plenum 1981, Chap. 2.
- ¹⁷S. V. Vonsovskii, Yu. A. Izyumov, and E. Z. Kurmaev, Superconductivity of Transition Metals, Their Alloys, and Their Compounds (in Russian), Nauka, 1977.
- ¹⁸O. V. Roitsina, Zh. Prikl. Spekt. **3**, 403 (1965).
- ¹⁹Yu. F. Momnik, Fiz. Nizk. Temp. **8**, 115 (1982) [Sov. J. Low Temp. Phys. **8**, 57 (1982)].
- ²⁰V. P. Volotskaya, V. A. Shklovskii, and L. E. Musienko, *ibid.* **6**, 1033 (1980) [6, 503 (1980)].
- ²¹R. A. Vardanyan and B. I. Ivlev, Zh. Eksp. Teor. Fiz. **65**, 2315 (1973) [Sov. Phys. JETP **38**, 1156 (1974)]. G. M. Eliashberg, Pis'ma Zh. Eksp. Teor. Fiz. **11**, 186 (1970) [JETP Lett. **11**, 114 (1970)].
- ²²M. E. Gershenzon, V. N. Gubankov, and Yu. E. Zhuravlev, Zh. Eksp. Teor. Fiz. **85**, 287 (1983) [Sov. Phys. JETP **57**, 167 (1983)].
- ²³B. I. Ivlev, N. B. Kopnin, and L. A. Maslova, *ibid.* **78**, 986 (1980) [51, 986 (1980)].
- ²⁴A. Schmid, Proc. NATO Adv. Study Inst. **65**, Chap. 14, 1980.
- ²⁵A. V. Gurevich and R. G. Mints, Pis'ma Zh. Eksp. Teor. Fiz. **31**, 52 (1980) [JETP Lett. **31**, 48 (1980)].

Translated by J. G. Adashko